Novel solutions for closed-loop Reverse Electrodialysis: thermodynamic characterisation and perspective analysis

Novel solutions for closed-loop Reverse Electrodialysis: thermodynamic characterisation and perspective analysis

F. Giacalone[a,b], C. Olkis[a], G. Santori[a], A. Cipollina[b,**], S. Brandani[a,*] G. Micale[b]

[a]*The University of Edinburgh, School of Engineering, Institute for Materials and Processes, Sanderson Building, The King's Buildings, Mayfield Road, EH9 3JL Edinburgh, Scotland, UK.*
* S.Brandani@ed.ac.uk

[b]*Dipartimento dell'Innovazione Industriale e Digitale (DIID), Ingegneria Chimica, Gestionale, Informatica e Meccanica, Università degli Studi di Palermo (UNIPA)- viale delle Scienze Ed.6, 90128 Palermo, Italy.*
**andrea.cipollina@unipa.it

Abstract

Closed-loop Reverse Electrodialysis is a novel technology to directly convert low-grade heat into electricity. It consists of a reverse electrodialysis (RED) unit where electricity is produced exploiting the salinity gradient between two salt-water solutions, coupled with a regeneration unit where waste-heat is used to treat the solutions exiting from the RED unit and restore their initial composition. One of the most important advantages of closed-loop systems compared to the open systems is the possibility to select ad-hoc salt solutions to achieve high efficiencies. Therefore, the properties of the salt solutions are essential to assess the performance of the energy generation and solution regeneration processes. The aim of this study is to analyse the influence of thermodynamic properties of non-conventional salt solutions (i.e. other than NaCl-aqueous solutions) and their influence on the operation of the closed-loop RED. New data for caesium and potassium acetate salts, i.e. osmotic and activity coefficients in aqueous solutions, at temperature between 20 and 90°C are reported as a function of molality. The data are correlated using Pitzer's model, which is then used to assess the theoretical performance of the whole closed-loop RED system considering both single and multi-stage regeneration units. Results indicate that KAc, CsAc and LiCl are the most promising salts among those screened.

Keyword: *Closed loop reverse electrodialysis, multi-stage evaporative regeneration unit, potassium acetate, caesium acetate, osmotic coefficient, Pitzer's model.*

1 Introduction

Salinity Gradient Power (SGP) is a renewable energy originating by mixing two salt solutions at different concentrations. Currently, three different technologies are proposed to exploit such energy: Pressure Retarded

Osmosis (PRO) [1,2],Reverse Electrodialysis (RED) [3,4] and CAPacitive MIXing (CAPMIX) [5]. Conventional open-loop SGP technologies exploit natural salinity gradients, e.g. river water and seawater. In recent years, the application of SGP in closed-loop has gained attention in the scientific community. SGP in closed loop may be regarded as an integrated system where one of the SGP processes (i.e. PRO, RED or CAPMIX) is coupled with a thermal regeneration process in which waste heat is used to restore the initial condition of the saline solutions exiting from the SGP unit [6].

The most interesting aspect in closed-loop operation is the possibility to select an ad-hoc saline solution to enhance the overall performance of the integrated process. A mindful choice of the artificial saline solution ensures (i) the availability of large amounts of Gibbs free energy of mixing, (ii) low energy consumption in the regeneration unit to restore the original concentration levels of feed solutions, (iii) use of waste heat at low temperature. Waste heat is a widely available source. It has been estimated that the waste heat potential in EU is ~110 TWh/y, about of 50% of which is represented by waste heat at temperature level below 200°C [7].

Depending on the choice of the artificial saline solution, a variety of different processes can be developed for the regeneration stage. These can be grouped in two main categories: (i) *solvent extraction processes* and (ii) *salt extraction processes*. *Solvent extraction processes* make use of waste heat in order to transport solvent from the exhausted concentrate stream to the exhausted dilute one. In this case, different evaporative processes may be used, such as Multi Effect Distillation (MED)[8], Membrane Distillation (MD)[9] or Adsorption Desalination (AD)[10]. Conversely, salt extraction processes move the salt from the exhausted dilute to the exhausted concentrated solution. In this case, a promising option is the use of thermolytic salts, which decompose in gaseous species when increasing the temperature of the solution above the salt decomposition temperature, thus being easily separated by a stripping unit [11].

Among all the strategies proposed, this work is focused on SGP closed-loop system in which a RED unit is coupled with a generic solvent-extraction evaporative process. Reverse electrodialysis is a membrane-based process able to convert the salinity gradient between a concentrate and dilute ionic solution into electricity. A typical RED stack consists of an alternating series of Cation Exchange Membranes (CEMs) and Anion Exchange Membranes (AEMs) placed between two electrodes. The membranes are typically separated by

mechanical spacers, which ensure stability of the channels where the two solutions are fed in an alternating fashion. In this way cations and anions are forced to move from the concentrate channel to the adjacent dilute one, although in opposite directions. Electrodes are located at both ends of the stack where redox reactions take place, converting the ionic flux into an electronic flux (i.e. an electric current). As a result, the two outlet solutions have lost their original concentration level, thus requiring a regeneration step in order to be reused as a feed for the RED process. In a solvent-extraction evaporative regeneration unit, waste heat is used to evaporate part of the solvent from the concentrate stream, restoring the initial concentration of salt. The produced solvent is mixed with the dilute solution to restore its initial concentration. The primary performance indicator relevant to the thermally driven evaporative process is the specific thermal consumption and the operating temperature, which affect the exergetic and energetic efficiency of the integrated system. These parameters depend on several aspects such as process configuration (e.g. single stage or multi stage) and solution properties (e.g. Boiling Point Elevation, Heat of vaporization, Specific Heat).

The selection of the most suitable salt solution must take into account a number of factors, which characterize the closed-loop system. The optimal salt for RED should have (i) high solubility in water, (ii) high salt activity coefficients at high concentrations and (iii) high conductivity. The solubility and the activity coefficients strongly influence the RED process performance in terms of electro-motive force (e.m.f.) and consequently the power density, but also the energy density (or Gibbs free energy of mixing, kWh/m^3) As an example, the solubility of sodium chloride (NaCl) in water is 6.15 molar (26.45 gr. salt/100 gr. solution) at 25°C [12], while the e.m.f. is around 0.2V per cell-pair when a saturated NaCl solution is mixed to a dilute one (0.05M) [13]. Other inorganic salts, such as lithium chloride (LiCl), lithium bromide (LiBr), caesium acetate (CsAc), potassium acetate (KAc), have a remarkably higher solubility [14,15], allowing, in principle, to obtain much larger values of Gibbs free energy of mixing.

Solution conductivity is another important property, as it affects the electrical resistance of the two solutions. In particular, the dilute channel electrical resistance represents the most important contribution to the overall stack internal electrical resistance [16].

As reported by Tamburini et al. [13] the use of non-conventional salt solutions can result in values of e.m.f. and power density significantly higher than conventional NaCl solutions. In particular, the use of the above mentioned salts (LiCl, LiBr, KAc and CsAc) can lead to values up to 6 times higher [13].

For the evaporative regeneration step an optimal salt solution must have low Boiling Point Elevation (BPE) and low enthalpy of vaporization. The enthalpy of vaporization influences the heat consumption of the evaporative unit, while the BPE affects the temperature of the heat source required and can limit the number of stages of a multi-stage evaporative process [8]. The latent heat depends mainly on the solvent nature. Water is the most used solvent, while organic solvents provide a lower latent heat. Therefore, the use of organic solvents can theoretically reduce the specific energy consumption but, due to low salt solubility, low solution conductivity and reduced compatibility with the membrane material, the power production is negatively affected so that the choice of such solvents is not viable. The BPE depends on the nature of the salt and on its concentration.

Recent studies on closed loop reverse electrodialysis using solvent extraction regeneration unit have been mainly focused on modelling analyses of the system using conventional NaCl aqueous solutions. In particular, Tamburini et al. [13] analysed the performance of a RED-MED HE adopting a very simplified modelling approach. Results indicated a maximum electrical generation efficiency of 5% (27.9% exergy efficiency) using current state of the art systems, while efficiency around 15.4% (86% exergy efficiency) may be obtained in future scenarios, thanks to system's improvements. Long et al. [17] carried out a parametric study on a hybrid MD-RED system, indicating a maximum electrical generation efficiency of 1.15%. Hu et al. [18] performed a detailed theoretical analysis on the performance of a hybrid MED-RED heat engine. A maximum electrical generation efficiency of 1% was found coupling a RED unit with a 10 effects MED unit powered by low grade heat at 95 °C.

To further explore the potentials of closed-loop RED technology, however, such analysis should not be limited to the use of conventional NaCl salt solutions. At the contrary, the study of system performance with non-conventional (i.e. ither than NaCl) salts solution could lead to significant performance enhancements, opeing room for further deveoplemnts of this technology. To this aim, detailed information about thermodynamic

properties of novel electrolyte solutions is needed, though such kind of information is often not fully available in the literature.

The thermodynamic characterization of salt aqueous solutions requires the calculation of osmotic and activity coefficients in solution. The most accurate approach is the ion interaction model of Pitzer [19], where the model parameters describing the interaction of ions in solution have to be determined from experimental data. For common salts like NaCl [20], LiCl [21,22], KCl [23], several data are published in the literature but only few thermodynamic data are available for less common salts such as the acetate salts. These salts show interesting properties, which make them suitable for utilization in closed-loop RED system. Beyer and Steiger [24] carried out experiments for the determination of the Pitzer's model parameters of sodium acetate (NaAc). They measured partial pressures and evaluated the corresponding osmotic coefficients from a temperature of 278.15 K to 313.15 K and a molality of 0.65 mol/kg_s to 6.47 mol/kg_s. Equilibrium data of potassium and caesium acetates have been measured in a small range of concentrations (from 0.1 to 3.5 mol/kg_s) at 298 K [25–27] and further investigation is needed to extend this range.

This work focuses on (i) the collection of novel thermodynamic data on CsAc and KAc and (ii) the analysis of the influence of thermodynamic properties (i.e. osmotic and activity coefficients) of NaCl, LiCl, NaAc, CsAc and KAc water solutions in a closed-loop RED system. A specific measurement cell was developed to assess the boiling point elevation of LiCl NaCl and the above-mentioned acetate salts. The new vapour pressure measurements were used with available literature data to regress Pitzer's model parameters which allow to describe the osmotic and activity coefficients of potassium and caesium acetates in a wide range of temperature (20-90°C) and molality (up to 9 molal). The calculated osmotic and activity coefficients for KAc CsAc, LiCl, NaAc and NaCl, were used to evaluate and compare the different Gibbs free energies of mixing and the thermal energy consumptions coupled with the maximum number of stages practicable in a multi-stage evaporative regeneration. Finally, also thermal and exergy efficiencies of the closed-loop RED system were analysed.

2 Thermodynamics of electrolyte solutions

When an electrolyte is in contact with a polar solvent (e.g. water) a solvation process occurs: the solvent molecules (dipoles) interact with the ions, orienting themselves in the direction of the electric field and reducing the electrostatic force of the electrolyte lattice. As result of the solvation process, the electrolyte is separated into cations and anions uniformly disperse in the solvent. Due to the ion-ion and ion-solvent interactions, the behaviour of the solvent and solute in an electrolyte solution deviates from the ideal case when solute concentration increases. These deviations are thermodynamically accounted by means of *activity coefficients* for ions and solvent.

The chemical potential of individual ionic species (μ_i) can be written as:

$$\mu_i = \mu_i^0 + RT \ln a_i \quad (1)$$

in which a_i is the activity of the i^{th} ion in the solution and μ_i^0 is the chemical potential of the i^{th} ions in the standard state (J/mol), T is the absolute temperature (K) and R=8.3144 J/ (mol K) is the universal gas constant. Thermodynamic measurements yield properties of the solute and not of individual ionic species. Thus, the chemical potential for a generic electrolyte (*MX*) is given by:

$$\mu_{MX} = \mu_{MX}^0 + \nu RT \ln(m_{\pm}\gamma_{\pm}) \quad (2)$$

The μ_{MX}^0 term is a combination of the chemical potentials of the two ions in the standard state (J/mol), $\nu = \nu^+ + \nu^-$ is the number of ions generated by the complete dissociation of the salt, $m_{\pm}$(mol/kg$_s$) and $\gamma_{\pm}$ are the geometrical average of molality and activity coefficient of the two ions (coinciding with salt's ones for the case of monovalent salts). It is worth mentioning that the reference state for the solute is that of infinite dilution in the solvent, i.e. $\gamma_{\pm} \to 1$ as $m_{\pm} \to 0$.

For the generic solvent, the chemical potential is defined as:

$$\mu_s = \mu_s^0 + RT \ln a_s \quad (3)$$

in which a_s is the solvent activity and μ_s^0 is the solvent chemical potential in the standard state (J/mol). For the solvent the normal reference state is used, i.e. that of the pure liquid at the same temperature and pressure of

the mixture. Pressure effects are negligible and therefore no Poynting correction factors are needed.

The solvent activity in electrolyte solutions is given by the ratio of the solution fugacity (f_s) (bar) and pure water fugacity(f_s^0) (bar) at the saturation temperature:

$$a_s = \frac{f_s}{f_s^0} \tag{4}$$

If ideal behaviour in gas phase is assumed, equation (4) simplifies to:

$$a_s = \frac{p_s}{p_s^0} \tag{5}$$

where p_s and p_s^0 are the solution vapour pressure and the pure water vapour pressure (bar), respectively. Equation 5 links measurable properties (i.e. vapour pressure measurements) to the activity of the solvent and the osmotic coefficient ϕ, which characterise the deviation of a solvent from ideal behaviour. The osmotic coefficient is related to the activity coefficient according to:

$$\phi = \frac{-1000\, ln\, a_s}{MW_s \sum_i \nu_i m_i} \tag{6}$$

where MW is the molar mass of the solvent (g/mol), m_i is the electrolyte molality in the solution (mol/kg), ν_i is the number of each i^{th} ions generated by the complete dissociation of the salt.

The osmotic coefficient and the activity coefficient are related by the Gibbs-Duhem equation [1,13], which eventually leads to the following relationship:

$$-\ln \gamma_{\pm} = \int_{m=0}^{m} (1-\phi) d \ln \mathrm{m} \tag{7}$$

2.1 Pitzer's Model

In the Pitzer's model, the long-range interactions between the charges are described using the Debye-Huckel term, while the short-range interactions are modelled using an empirical virial expansion. The coefficients of this expansion are the virial coefficients. The second virial coefficient is expressed in terms of the parameters $\beta_{MX}^{(0)}$, $\beta_{MX}^{(1)}$, while the third virial coefficient is C_{MX}^{ϕ}. The osmotic and salt activity coefficients can be calculated from the following equations, which are consistent with the Gibbs-Duhem relationship, eq. (7):

$$\phi - 1 = |z_M z_X| f^{\phi} + \frac{m}{m_0}\left(\frac{2\nu_M \nu_X}{\upsilon}\right) B_{MX}^{\phi} + \frac{m^2}{{m_0}^2} \frac{2(\nu_M \nu_X)^{1.5}}{\upsilon} C_{MX}^{\phi} \tag{8}$$

$$ln\,\gamma_{\pm} = |z_M z_X| f^{\gamma} + \frac{m}{m_0}\left(\frac{2\nu_M\nu_X}{\upsilon}\right) B^{\gamma}_{MX} + \frac{3m^2}{2{m_0}^2}\frac{2(\nu_M\nu_X)^{1.5}}{\upsilon} C^{\phi}_{MX} \quad (9)$$

with

$$f^{\phi} = -A_{\phi}\frac{I^{0.5}}{1+bI^{0.5}} \quad (10)$$

$$f^{\gamma} = -A_{\phi}\left[\frac{I^{0.5}}{1+bI^{0.5}} + \frac{2}{b}\ln(1+bI^{0.5})\right] \quad (11)$$

$$B^{\phi}_{MX} = \left[\beta^{(0)}_{MX} + \beta^{(1)}_{MX}\exp(-\alpha I^{0.5})\right] \quad (12)$$

$$B^{\gamma}_{MX} = 2\beta^{(0)}_{MX} + \frac{2\beta^{(1)}_{MX}}{\alpha^2 I}\left[1 - \left(1+\alpha I^{0.5} - \frac{\alpha^2 I}{2}\right)\cdot\exp(-\alpha I^{0.5})\right] \quad (13)$$

in which ν_M, ν_X, z_M and z_X are the number and the charge of positive and negative ions, respectively, m_0 = 1 mol·kg^{-1} is the standard molality, b = 1.2 kg$^{1/2}$·mol$^{-1/2}$ is a universal parameter; α is a numerical constant equal to 2 for univalent ions; I is the ionic strength (mol/kg$_s$) and A_{ϕ} is the Debye-Huckel parameter for the osmotic coefficient. This is related to the long-range forces and depends on solvent type, temperature and pressure, according to equation (14).

$$A_{\phi} = \frac{1}{3}\left(\frac{2\pi N_0\rho_w}{1000}\right)^{\frac{1}{2}}\left(\frac{e^2}{4\pi\epsilon_0\epsilon kT}\right)^{\frac{3}{2}} \quad (14)$$

with N_0 Avogadro's number (kmol^{-1}), ρ_w the density of the water (kg/m^3), e the electron charge (C), k Boltzmann's constant (J/K), ϵ the relative permittivity of water [19,28], ϵ_0= 8.854187817×10^{-12} F·m^{-1} the permittivity of free space, and T the absolute temperature (K).

$\beta^{(0)}_{MX}$, $\beta^{(1)}_{MX}$ and C^{ϕ}_{MX} are salt specific parameters and can be obtained regressing experimental data of osmotic coefficients or from vapour pressure measurements.

2.2 The Gibbs free energy of mixing

The maximum amount of work obtainable from any SGP technology is given by the Gibbs free energy of mixing. When a solution at high concentration is mixed with a solution at low concentration, the resulting effect is a variation of the Gibbs free energy of the system, i.e. the Gibbs free energy of mixing, which may

ideally be converted in electricity when no dissipative phenomena are involved in the recovery process [29]. The Gibbs free energy of a generic salt aqueous solutions is defined as:

$$G_i = n_{MX,i}\,\mu_{MX,i} + n_s\,\mu_{MX,s} = n_{MX,i}\,[\mu^0_{MZ,i} + \nu RT\,ln(\,m_{\pm,i}\,\gamma_{\pm,i})] + n_s\,[\mu^0_{s,i} + RT\ln(a_{s,i})] \quad (15)$$

where $n_{MX,i}\,\mu_{MX,i}$ are the product of the salt moles (mol) by the salt chemical potential (J/mol) and $n_s\,\mu_{MX,s}$ are the product of the water moles (mol) by the water chemical potential (J/mol). The Gibbs free energy of mixing is evaluated as the difference between the Gibbs free energy of the solution resulting (G_{mix}) from the mixing and the Gibbs free energy of the two original solutions (i.e. G_{low} and G_{high}):

$$\Delta G_{mix} = (G_{mix} - G_{low} - G_{high}) \quad (16)$$

The Gibbs free energy of mixing (ΔG_{mix}) is evaluated considering both salt and solvent influence on the chemical potential. However, when streams at low concentration are considered (as in the case of natural streams like seawater and river water) the contribution of water can be neglected, thus simplifying equation (16) by deleting the last term [30]. Conversely, when streams have high salt concentration (as in the case of saturated brines and in closed loop applications) the effect of water can be significant in the determination of the free energy of mixing and all terms have to be considered. This is highlighted in Figure 1 for NaCl solutions at fixed dilute concentration of 10^{-6} mol/kg$_s$.

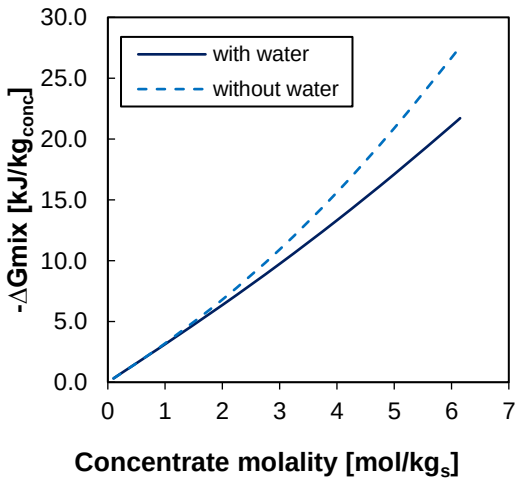

Figure 1. *Gibbs free energy of mixing as a function of concentrate NaCl solutions molarity at 25°C calculated neglecting the effect of water on the chemical potential (without water, blue dashed-line) and including it (with water, blue line). Dilute molality set at 10^{-6} mol/kg$_s$. and equal amount of solutions (1 kg) mixed.*

2.3 Boiling point elevation in electrolyte solutions

The thermal energy consumption (TEC) of the regeneration unit, defined as the thermal energy required to restore the concentration of the two solutions exiting from the RED unit, depends on heat of vaporization and boiling point elevation (BPE) (especially when multi-stage approaches are used). In particular, assuming similar heat of vaporization for salt solutions with the same solvent (e.g. water), the main effect of the salt consists of an increase (at fixed pressure) of the boiling temperature of the solution compared with the pure solvent (BPE). In this study, experimental values of BPEs are evaluated from vapour pressure measurements of salt solutions at different concentrations and temperatures.

In fact, BPE is related to the activity of the solvent in the solution and thus to the osmotic coefficient. The relevant equations used to evaluate the BPE via Pitzer's model are reported below.

$$BPE = T_{sol}^{eb}(p_s, m) - T_{pure}^{eb}(p_s) \quad (17)$$

where p_s is derived from equations (5,6 and 8):

$$p_s = p_s\left(m, T_{sol}^{eb}\right) = \exp\left[-\frac{\phi\,(m,T_{sol}^{eb})}{1000} MW_s\; m\; v\right] \cdot p_w(T_{sol}^{eb}) \quad (18)$$

For a given p_s the boiling temperature of pure water (T_{pure}^{eb}) or its vapour pressure (p_w) can be evaluated using the Saul and Wagner equation [31]. The actual calculation procedure for BPE starts from fixing a value of T_{sol}^{eb}, from which determining p_s (eq. (18), after fixing a value for *m*) and, eventually, T_{pure}^{eb} (at p_s), thus obtaining the value of BPE from eq.(17).

3 Experimental setup and procedure

3.1 Experimental setup

A schematic representation of the test-rig used to evaluate the partial pressure of salt solutions is shown in Figure 2. The main element of the system is a static cell consisting of a glass flask equipped with a thermal jacket, fed with water from a thermal bath which maintains the solution at a controlled temperature measured with a T-Type thermocouple.

The cell is provided with a glass arm, where the vacuum line and the pressure transducer are connected. The vacuum line is equipped with (i) a regulating valve, (ii) a cold trap, and (iii) a vacuum pump. The glass tube connecting the sample flask to the pressure gauge was insulated and maintained at T = 90 °C with a heating tape to avoid vapour condensation. The solution in the sample flask was agitated during the measurement with a magnetic stirrer. Details of the experimental apparatus components are reported in Table 1.

Calibration of the system was carried out using pure de-ionized water to determine the temperature offset between the measured temperature and the temperature in the liquid phase. See appendix A.1 for details.

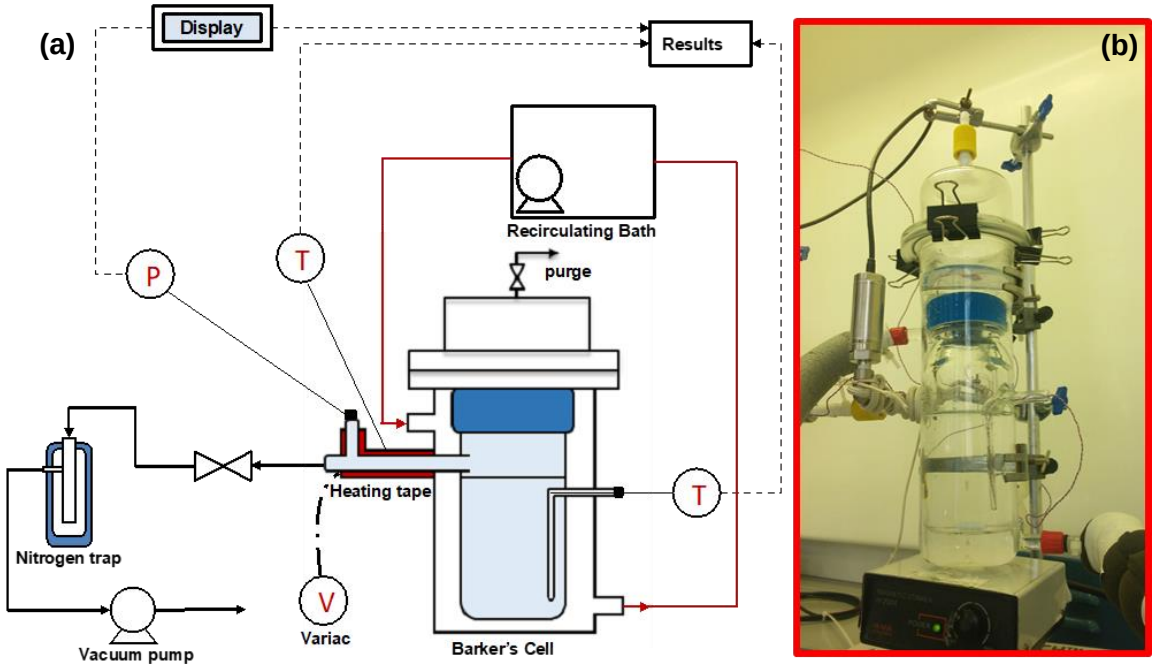

Figure 2. *Schematic representation of the test-rig (a) and picture of the static cell (b)*

Table 1. *Specification of the experimental apparatus equipment and reagents.*

Components	Specifications
Pressure Transducer	General Electric UNIK5000, accuracy: ± 0.165 kPa
Thermal bath	Julabo Corio CD-300F, temperature stability: ±0.03 °C, resolution: ±0.1 °C
Thermocouples	RS Pro Type T Thermocouple Copper probe 814-0153, accuracy: ±0.1 °C
Heating tape	Electrothermal MC5
Vacuum pump	Edwards nXDS 6i
Magnetic stirrer	Hanna Instruments HI 200M
Balance	Mettler Toledo XS205 DualRange, accuracy: ±0.01 mg (0-81 g) and ±0.1 mg (0-220 g)
Sodium Acetate (NaAc)	Sigma Aldrich, purity ≥99.0%
Potassium Acetate (KAc)	Sigma Aldrich, purity ≥99.0%
Caesium Acetate (CsAc)	Sigma Aldrich, purity >99.9%
Lithium Chloride (LiCl)	Sigma Aldrich, purity 99.0%
Sodium Chloride (NaCl)	Sigma Aldrich, purity ≥99.0%
De-ionised water	Elga Centra R200

3.2 Test preparation

Solutions were prepared using anhydrous salt (analytical grade, purity > 0.99, Sigma-Aldrich) and de-ionised water (more details are reported in Table 1). The salt was dried at T = 393 K for 1 week until no mass variation was detected. The solution was prepared weighing separately the salt and the water. For each test, the salt was dissolved in 250 g of water at room temperature and the solution was then loaded in the cell for the test.

Before cell loading, the sample solution is degassed with a sonic bath to remove air bubbles, then the solution was loaded inside the cell, making sure that its level is under the glass arm.

All the dissolved and gaseous air present in the cell was evacuated before running the experiment. Vacuum was obtained in two steps: the measurement cell (step 1) was cooled to 10°C in order to pull the vacuum at a temperature in which the solvent vapour pressure is reasonably low. Opening the vacuum valve, the pressure of the cell decreased until a constant value. Then, the valve was closed and the pressure inside the cell increased due to the degassing of the dissolved air present in the solution and some evaporation of the solvent. The cell (step 2) was heated to 50 °C to facilitate the degassing process. When this condition was achieved the valve was opened briefly to evacuate the gas. After this, step 1 was repeated to achieve a good vacuum level. Any solvent evaporated during these steps was condensed in the liquid nitrogen trap and this amount of liquid was measured and the concentration of the solution corrected accordingly.

3.3 Test procedure

Starting from a temperature of 293.15 K, a stepwise increase of 10 K was adopted to reach a final temperature

275 of 363.15 K, always ensuring the attainment of vapour-liquid equilibrium.

276 To test the experimental apparatus and procedure, experimental measurements of vapour pressures for three
277 different salt-water solutions (NaCl, LiCl and NaAc) were carried-out. The resulting activities were converted
278 to osmotic coefficients and compared with literature data. The details of this validation are reported in the
279 appendix A.1, while new data obtained for CsAc and KAc are reported in the following section.

280

4 Thermodynamic characterization of KAc and CsAc solutions.

Vapour pressure measurements for KAc- and CsAc-water solutions were used to evaluate the corresponding osmotic coefficients (eqs. 5-6), which are reported in Figure 3 as a function of molality and temperature. For all the investigated salt-water solutions, the osmotic coefficients increase with the molality of the solution. The temperature dependence of the osmotic coefficient significantly changes with salt type and molality (see also the appendix A.1).

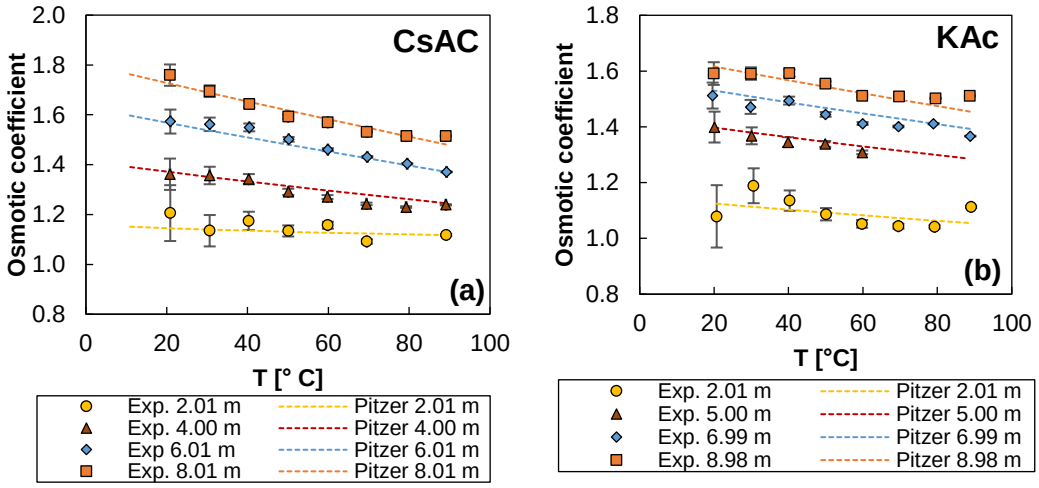

Figure 3.*Comparison between calculated and experimental osmotic coefficient for caesium acetate (a) and potassium acetate (b) as a function of temperature and solution molality.*

In order to fit the experimentally evaluated osmotic coefficients (reported in Figure 3) using Pitzer's model (eqs. 8, 10 and 12), the virial coefficients were evaluated using the following correlations (eq. 19-21).

$$\beta_{MX}^{(0)} = b_{01} + b_{02}T \tag{19}$$

$$\beta_{MX}^{(1)} = b_{11} + b_{12}T \tag{20}$$

$$C_{MX}^{\phi} = c_1 + c_2T \tag{21}$$

where b_{0i} , b_{1i} and c_i are fitting parameters. The simple linear temperature dependence of the parameters is used here since it provides a fit that is within the experimental uncertainty and also because it allows for moderate extrapolation beyond the range of measurements.

A comparison of osmotic coefficient obtained from experimental measurements of vapour pressure (eqs. 5 and 6) and calculated ones (eq. 8), is depicted in Figure 3.a-b. The fitting parameters adopted in eqs 19-21 are summarized in Table 2. In the same table, the root-mean-square error (RMSE), which is the difference between predicted values and actual values of φ, is reported.

Table 2. *Fitting parameters adopted to calculate the virial coefficients for CsAc and KAc.*

	CsAc	KAc
b_{01}	0.3292	0.2044
b_{02}	$-5.523\cdot10^{-04}$	$-1.662\cdot10^{-04}$
b_{11}	–2.924	0.3611
b_{12}	0.0110	-
c_1	–0.0122	–0.0067
c_2	$2.176\cdot10^{-05}$	-
RMSE	0.0237	0.0084

Previous studies on Potassium and Caesium acetate aqueous solutions [25,26] are available only at 298.15 K and limited to a maximum molality of 3.5 mol/kg$_s$. The parameters presented in this work extend the range of applicability of the Pitzer's equations for both temperatures, i.e. between 20 and 90°C, and molality, i.e. 8 mol/kg$_s$ in the case of CsAc and 9 mol/kg$_s$ in the case of KAc. A validation with literature data is reported in Figure 4 at 25°C, as a function of molality.

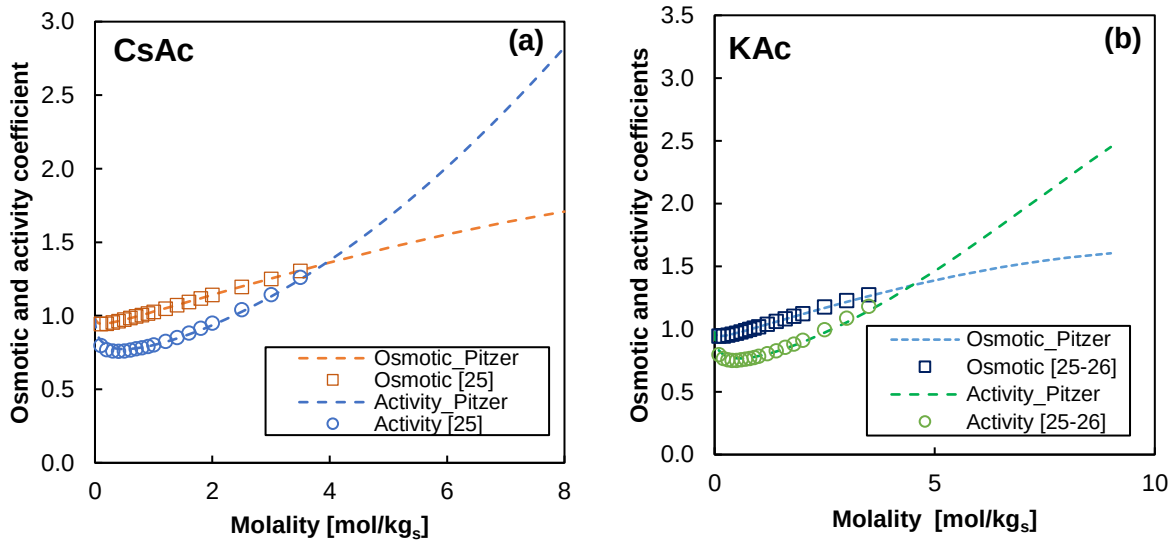

Figure 4.*Comparison of calculated salt activity and osmotic coefficient for CsAc (a) and KAc (b) and literature information* [25,26] *as function of solution molality at 25°C.*

A comparison of experimental BPEs and the ones calculated via Pitzer's model (see eqs. 17 and 18), as a function of the solution boiling temperature and salt solution molality, is reported in Figure 5 for CsAc and KAc, while in appendix for the other studied salts (Appendix A.2). The square markers represent the experimental values while dashed curves refer to model calculations. For all salts and conditions, experimental and calculation BPE are in excellent agreement.

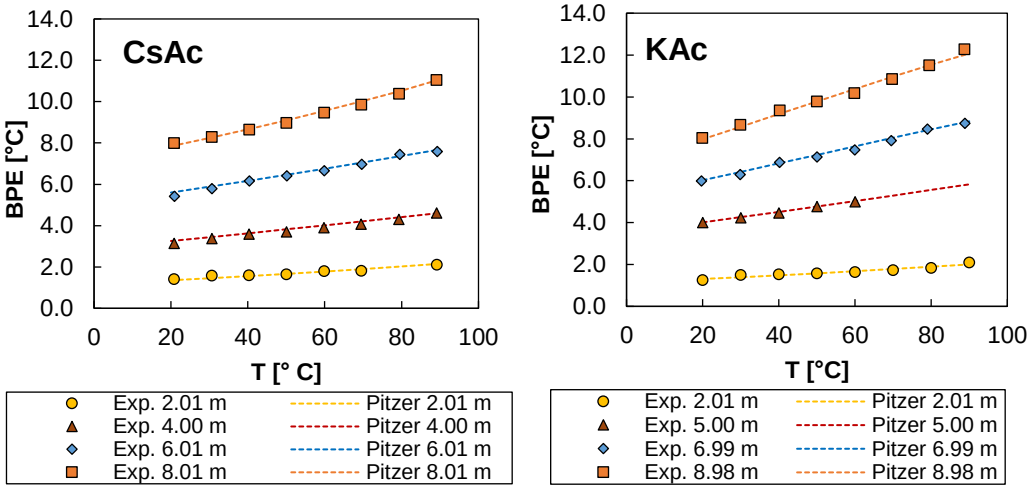

Figure 5. *Calculated and experimental BPEs as function of molality and temperature for CsAc and KAc.*

5 Theoretical analysis of closed-loop RED with new saline solutions

The parameters and correlations for evaluating the virial coefficients of KAc and CsAc were used to assess their osmotic and activity coefficients via Pitzer's model and the corresponding BPE. Such information is used to evaluate the Gibbs free energy of mixing of two reference solution and to make estimation of the thermal power required by a multi-stage evaporative regeneration unit for the studied salt-solutions. Finally, the theoretical thermal and exergy efficiency of a theoretical closed-loop SGP engine operating with such solutions are computed.

Energy from mixing electrolyte solutions: the Gibbs free energy of mixing

Figure 6 shows the Gibbs free energy of mixing as a function of the concentrate solution molality, fixing the dilute molality at 10^{-6} mol/kg$_s$ and considering the same amount of feed solutions (i.e. 1 kg of dilute and 1 kg of concentrate) at 25°C (typical working temperature of RED units).

The Gibbs free energy of mixing is a function of (i) salt activity coefficient and (ii) the number of salt moles contained in the solutions. At constant molality, the higher the salt activity coefficients of the concentrate, the higher the chemical potential available from mixing the solutions. Accordingly, more energy can be obtained using a controlled mixing process. On the other hand, for a given molality the moles of salt in 1 kg of solution is related to the molecular weight of the salt. The higher the molecular weight the lower the moles per kg of solution. For this latter reason, KAc which has a lower activity coefficient than CsAc and lower molecular weight gives higher Gibbs free energy. Among the considered salts, the most promising salt in terms of Gibbs free energy of mixing is LiCl which gives the highest potential, i.e. –120 kJ/kg_{high} at 17 mol/kg_s. Thanks to their remarkable solubility, also KAc and CsAc have relevant Gibbs free energy, –63 kJ/ kg_{high} and –55 kJ/ kg_{high} at 17 mol/kg_s, respectively, which makes them interesting salts for closed loop applications.

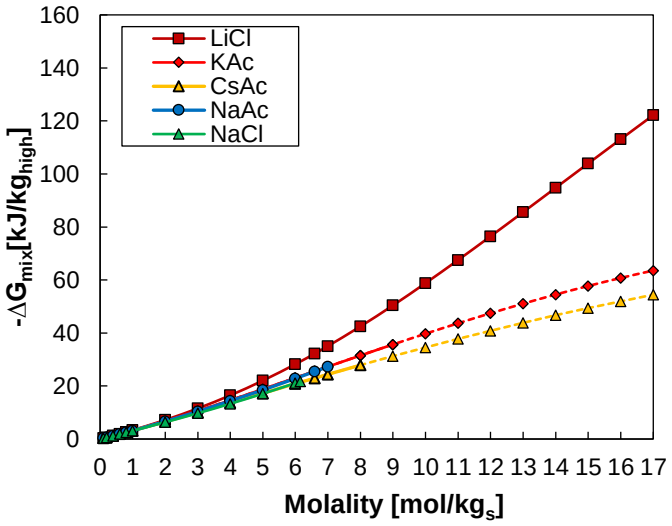

Figure 6. *Comparison of Gibbs free energy of mixing for NaCl, LiCl, NaAc, KAc and CsAc at 25°C and considering a dilute molality equal to 10^{-6} mol/kg_s. The concentration intervals, where the Gibbs free energy is calculated using extrapolated activity coefficients are indicated using dashed lines.*

5.1 Energy for regenerating electrolyte solutions: Thermal Energy Consumption (TEC) of single and multi-stage evaporative units.

The effect of the BPE on the performance of the regeneration unit is evaluated considering a simple model to describe the consumption of a single and multi-stage evaporative process. In both cases, the energy consumption of the regeneration unit is evaluated considering only the contribution of the energy required to evaporate the solvent, neglecting the sensible heat needed to heat up the solutions. Therefore, in a single-stage

regeneration unit the thermal energy consumption per unit of kg of solvent is equal to the solvent's latent heat of evaporation (for water λ_{ev}=2260 kJ/kg at 100°C). In a multi-stage regeneration unit, the thermal energy consumption depends on the number of stages adopted.

In a multi-stage unit, the regeneration of the solution is achieved dividing the vaporization process in several steps. Only the steam powering the first stage is generated using external energy source, while the other stages are powered by the vapour produced in the previous stage. The heat transfer from the condensing vapour to the evaporating brine is controlled by reducing the pressure along the stages, so that in each evaporative stage, the solvent reaches the boiling point at lower temperatures. In this way the thermal efficiency of the process is increased almost proportionally to the number of stages. The BPE often results as a limiting factor for a multi-stage regeneration unit of a RED closed loop system. In fact, the higher the BPE, the higher the temperature (i.e. pressure) drop required from one stage to the following in order to have a temperature driving force for heat transfer. Thus, the potential number of stages is reduced. For this reason, high values of BPE have a negative influence on the efficiency of multi-stage evaporative systems.

In order to quantify the effect of using different type and concentration of salt-water solution in a multi-stage regeneration unit, a simple model was developed to evaluate the minimum thermal power consumption, maximizing the number of stages.

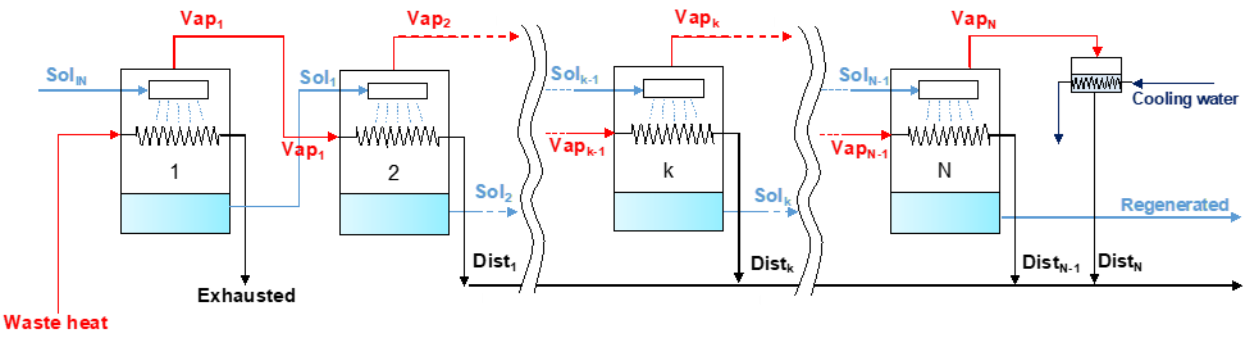

Figure 7. *Schematic representation of a multi-stage regeneration unit*

The calculation starts from the assumption of a fixed driving force (ΔT_{exch}) equal to 2°C, required in the heat exchanger to transfer the heat from the steam to the brine. The temperature of the solution in the k^{th} stage

($T_{sol,k}^{eb}$) is calculated subtracting ΔT_{exch} to the temperature of the condensing vapour obtained in the previous stage ($T_{vap,k-1}^{cond}$):

$$T_{sol,k}^{eb} = (T_{vap,k-1}^{cond}) - \Delta T_{exch} \quad (22)$$

In the first stage ($T_{vap,k-1}^{cond}$) is the temperature of the external waste heat fixed at 100°C. In each k^{th} stage the salt solution and the generated vapour are in equilibrium ($T_{sol,k}^{eb}$=$T_{vap,k}^{eb}$), but due to the BPE, a superheated vapour is produced. When reaching the following stage, the super-heated vapour cools down to the condensing temperature and, eventually, condensates by transferring the latent heat of condensation to the boiling brine. As an example, the temperature profiles (along the stages) of generated vapour, evaporating brine and condensing vapour in the subsequent stage is reported in Figure 8 for the case of a regeneration unit consisting of 4 stages and fed by a 4.6 mol/kg$_s$ solution of KAc. Then, the condensation temperature of the vapour in the k^{th} stage is calculated as:

$$T_{vap,k-1}^{cond} = T_{sol,k-1}^{eb} - BPE \quad (23)$$

where BPE is evaluated at the stage outlet brine molality.

The enthalpy of vaporization of the solvent ($\lambda_{ev,k}$) is a function of the boiling temperature of the solution according to the Watson's equation [32]:

$$\lambda_{ev,k} = \lambda_{ev,n}\left[\frac{T_c - T_{sol,k}^{eb}}{T_c - T_n^{eb}}\right]^{0.38} \quad (24)$$

where $\lambda_{ev,n}$=2260 kJ/kg, T_n^{eb}= 373 K are the normal latent heat and boiling temperature of pure water, while T_c= 647.3 K is the critical temperature of water.

The mass of solution exiting from the k^{th} stage ($w_{sol,k}^{out}$) is calculated as:

$$w_{sol,k}^{out} = w_{sol,k}^{in} - \frac{Q_k}{\lambda_{ev,k}} \quad (25)$$

Where $w_{sol,k}^{in}$ is the inlet mass of solution and Q_k the heat provided by the condensation of the vapour produced in the previous stage ($w_{vap_{k-1}}$) computed according to:

$$Q_k = w_{vap,_{k-1}} \cdot \lambda_{ev,k-1} \quad (26)$$

For the first stage Q_1 is the heat provided by the waste-heat and represents the TEC of the multi-stage regeneration unit.

The molality of the solution feeds in the first stage was evaluated considering the equilibrium concentration given by mixing 1 kg of concentrate solution (variable concentration from 0.1 to 17 mol/kg$_s$, or up to the solubility limit for less soluble salts) and 1 kg of dilute solution (m_{dil}=10^{-6} mol/kg$_s$). Fixing a feed solution molality, the TEC in the regeneration unit is evaluated by maximizing the number of stages to obtain the vaporization of 1 kg of solvent limiting the pressure of the solution in the last stage to a minimum of 0.05 bar.

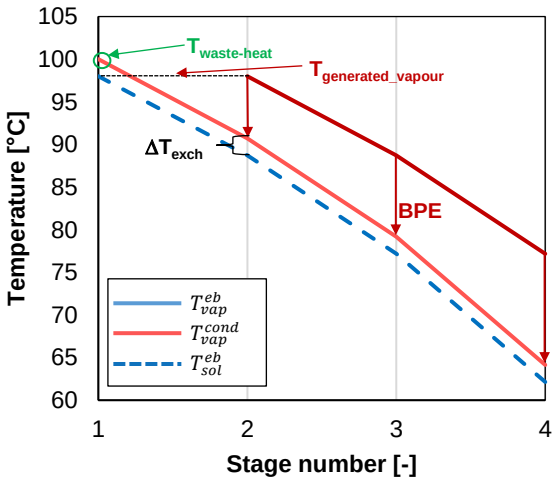

Figure 8.*Example of temperature profile of generated vapour in the previous stage ($T_{v,eb}$),condensing vapour ($T_{v,cond}$) and boiling solution ($T_{sol,eb}$) along the stages. KAc solution, inlet molality 4.63 mol/kg$_s$, outlet molality 17 mol/kg$_s$.*

A comparison of calculated BPEs of different salt aqueous solutions is reported in Figure 9. Figure 9.a, in particular shows BPEs as a function of the boiling solution temperature, fixing the solutions concentrations at 5 mol/kg. A linear dependence of BPEs from boiling temperature is observed for all the salts considered. In Figure 9.b BPEs are plotted as a function of solution molality, fixing the boiling temperature at 90°C. For NaAc and NaCl, BPE was calculated up to saturation molality, referring to the data reported in [12]. In the case of LiCl, KAc and CsAc, BPE was calculated up to a maximum molality of 17 mol/kg$_s$.

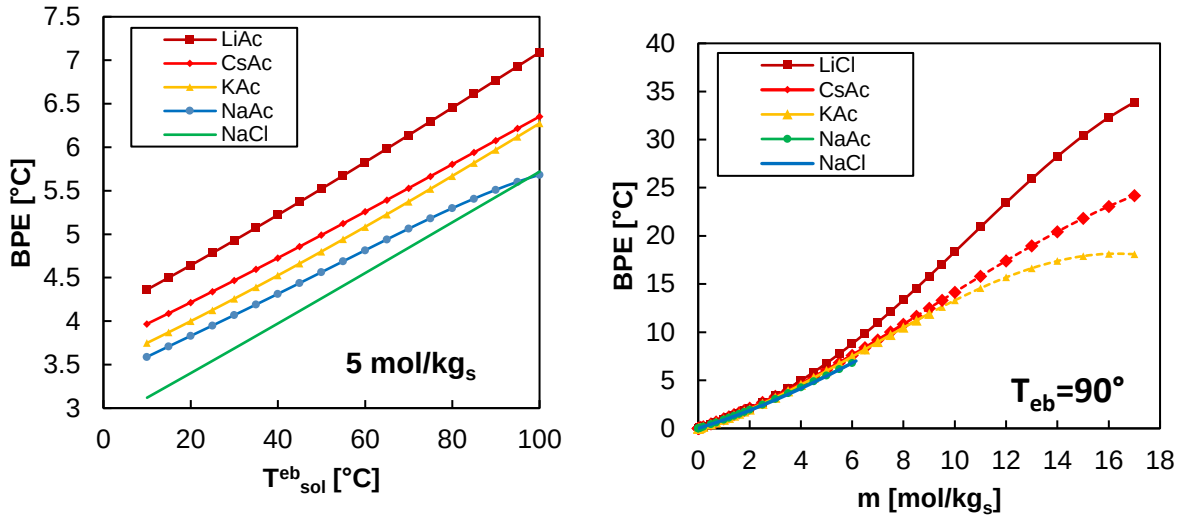

411

412 ***Figure 9.*** *Comparison of computed Boiling Point Elevation (BPE) for NaCl, LiCl, NaAc, KAc and CsAc water solutions*
413 *as a function of solution boiling temperature fixing the solution molality at 5 mol/kg$_s$ (a) and as a function of solution*
414 *molality (b) at 90°C. The concentration intervals, where the BPE is calculated using extrapolated osmotic coefficients*
415 *are indicated using dashed lines.*

416

417 Referring to LiCl, CsAc and KAc, for concentrations higher than 5 molal, the BPE increases rapidly with the
418 salt concentration. In the case of LiCl, at 90°C the BPE reaches values of about 18°C at 10 mol/kg$_s$ and of
419 34°C at 17 mol/kg$_s$. Relatively lower BPE values are observed for the two acetates (i.e. CsAc and KAc) ranging
420 between 13-14°C at 10 mol/kg$_s$ and between 18-25 °C at 17 mol/kg$_s$. For these salts at high concentration, the
421 ion-water and ion-ion interactions are so important that they largely affect the solution vapour pressure. In
422 these conditions, a thermally driven Regeneration Unit would require more thermal energy. In fact, the
423 possibility to adopt a multi-stage configuration to increase the thermal efficiency of the regeneration unit, is
424 limited to few stages.

425 Whit this respect, Figure 10.a reports the maximum number of stages for a multi-stage distillation unit used to
426 restore the original molality by evaporating 1 kg of water. When an outlet solution molality of 17 mol/kg$_s$ is
427 considered, the maximum number of stages is equal to 5 in the case of CsAc, 4 in the case of KAc while it is
428 reduced to 2 in the case of LiCl. The lower the number of stages, the higher the thermal power required, which
429 is equal to 1150 kJ in the case of LiCl, 585 kJ in the case of KAc and 480 kJ in the case of CsAc (Figure 10.b).

430 At lower molality values (i.e. 6 mol/kg$_s$) close to the saturation molality for NaCl and NaAc, the BPE reaches
431 maximum values around 6-9 °C for all salts. In this case, a thermally driven regeneration unit can work at

lower temperature compared to the previous case and if a multi-stage configuration is considered, more stages can be adopted (i.e. 9-12), with a corresponding TECs ranging between 200-280 kJ. In all cases, a TEC around 100 kJ is obtained when very low outlet molality is considered, i.e. 0.2 mol/kg_s, thanks to the adoption of 32 stages (maximum value considering a ΔT_{exch} of 2°C).

Reducing the ΔT_{exch}, results in an increase of the maximum number of stages and a decrease of thermal energy consumption in the regeneration unit, but on the other hand produces a dramatic increase of the heat transfer area required, thus making the scenarios technically and economically infeasible.

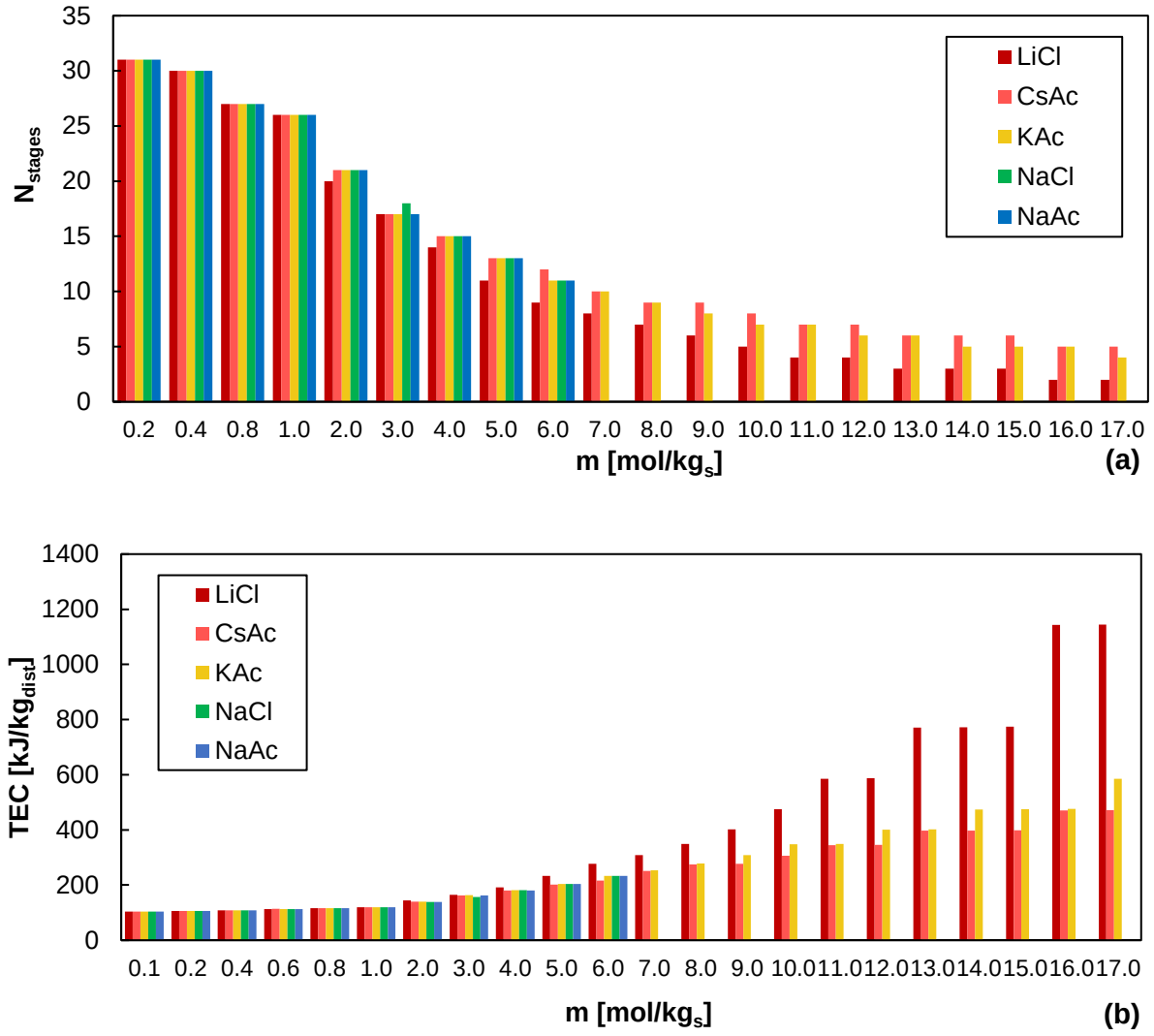

Figure 10. *Maximum number of stages (a) and TEC (b) of the MED unit as function of the regenerated solution. $T_{waste\text{-}heat}$=100°C, $p_{last} \geq 0.05$ bar ΔT_{exch}=2°C. Dilute molality=10^{-6} mol/kg_s.*

5.2 Thermal and Exergy Efficiency of the ideal RED engine

The effect of using different salt-solutions within a RED heat engine can be analysed looking at the global thermal efficiency for both single and multi-stage regeneration unit. The theoretical thermal efficiency of the global system using a single evaporative regeneration unit ($\eta_{th,single}$) is evaluated according to equation (27):

$$\eta_{th,single} = \frac{-\Delta G_{mix}}{TEC} = \frac{-\Delta G_{mix}}{2260\ kJ} \quad (27)$$

Which in the case of a multi-stage distillation process ($\eta_{th,multi}$) becomes:

$$\eta_{th,multi} = \frac{-\Delta G_{mix}}{TEC} = \frac{-\Delta G_{mix}}{Q_1} \quad (28)$$

The ratio of the thermal efficiency by the Carnot efficiency (η_c) gives the exergy efficiency:

$$\eta_{ex} = \frac{\eta_{th}}{\eta_c} \quad (29)$$

where η_c is evaluated between the lowest (298.15 K) and the highest (373.15 K) temperatures of the cycle.

It is worth noting that the maximum achievable energy of mixing has been assumed to compute the power output (as in [33]), though in practical applications such conditions might be not realizable [28].

The effect of using a different type of salt and solution molality on the theoretical thermal and exergy efficiency of the RED heat engine are reported in Figure 11.a for a single stage regeneration unit and in Figure 11.b in the case of a multi-stage distillation process. The thermal efficiency of the single stage system is a monotonic function of the solution molality. A similar results was obtained by Carati et al. [33], who performed a theoretical analysis of a SGP engine based on the use of $MgCl_2$, NaCl or NaOH solutions and adopting a single distillation unit for the regeneration. Also in that case, the highest efficiency was achieved for salts with the highest BPE, thanks to their highest Gibbs free energy of mixing.

In the case of less soluble salts, i.e. NaCl and NaAc, thermal and exergy efficiency maintain a monotonic behaviour also when a multi stage process is taken into account, because the increase in the Gibbs free energy with the solution molality prevails on the increase of the thermal energy consumption. For both salts (NaCl and NaAc) a maximum thermal efficiency around 10% is observed at 6 mol/kg_s using 11 effects. The thermal efficiency of the multi stage regeneration unit is ~10 times higher than the one of the single stage systems

when 6 mol/kg$_s$ concentrate solutions are regenerated.

Conversely, the efficiency of the multi stage system is not a monotonic function of the molality due to the balance of the two different contributions: (i) the increase of the Gibbs free energy of mixing and (ii) the decrease of the number of effects (or the increase of the TEC). As result, the highest thermal efficiencies around 13% are achieved for LiCl at 15 mol/kg$_s$ and 2 stages and for KAc at 16 mol/kg$_s$ and 5 stages. Slightly lower thermal efficiency of about 12.5% is obtained for CsAc at 15 mol/kg$_s$. Notwithstanding the Gibbs free energy of mixing of KAc and CsAc are remarkably lower than the one of LiCl, similar overall performance can be obtained from the three salts thanks to the adoption of a suitable multi-stage evaporative regeneration unit.

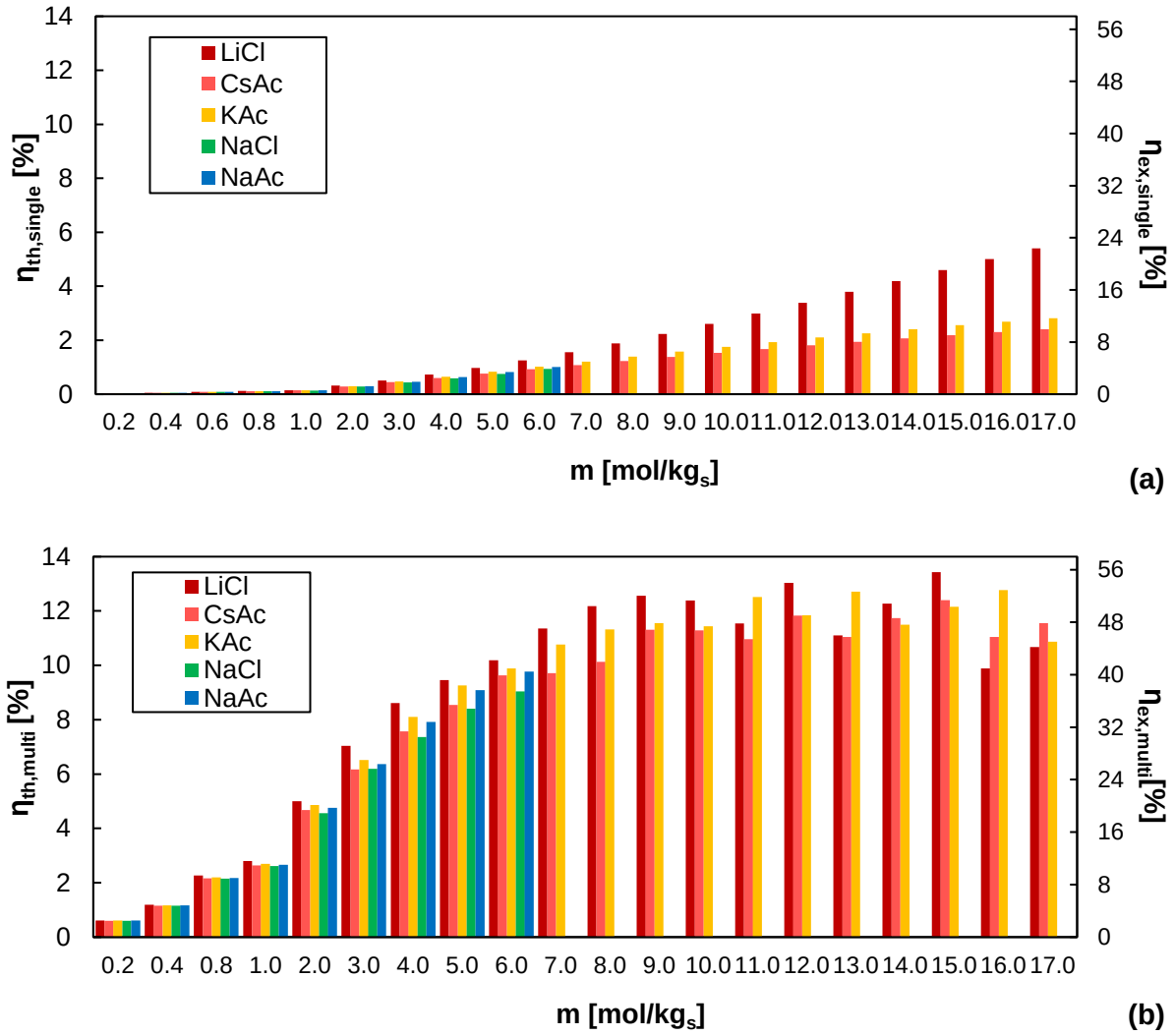

Figure 11. *Thermal and exergy efficiency for an ideal RED heat engine using a single stage (a) and in a multi stage regeneration unit. $T_{waste\ heat}$=100°C, $p_{last} \geq 0.05$ bar,, ΔT_{exch}=2°C. Dilute molality=10^{-6} mol/kg$_s$.*

Conclusions

Reverse electrodialysis in closed-loop system is a promising technology for converting low grade waste-heat into electricity. The adoption of a closed-loop allows the selection of different salt solutions. In particular, in this work, the possibility of using different salts from NaCl has been investigated.

An experimental campaign has been carried out in a purposely built laboratory set-up in order to characterise the thermodynamics of several salt solutions (LiCl, NaAc, CsAc and KAc) from solution vapour pressure measurements. Experimental data were used to determine the coefficients in Pitzer's model, which allow to evaluate activity and osmotic coefficients, as well as BPE, of all salt aqueous solutions. Compared to literature information, the novel data here obtained have allowed to extend the range of applicability of Pitzer's model in terms of temperature and molality for the case of CsAc and KAc.

Solubility, activity and BPE are the three thermodynamic features mostly affecting the performance of a RED-heat engine. The higher the salt solubility, the higher the BPE, but the lower the partial pressure of water in equilibrium with the solution. Thus, an optimal trade-off has to be identified between large chemical energy stored in the solution (depending on salt activity), which is released by the mixing process, and low energy requirements for the separation of the solvent for regeneration. The latter can be dramatically affected by high BPE where multiple-stage evaporation systems are adopted.

A theoretical analysis of the performance of an ideal RED-heat engine is presented, in which a regeneration with a single stage or multi stage evaporative process is considered. Results indicate how the use of acetate salts can lead to enhanced performances with respect to NaCl solutions, thanks to higher free energy of mixing and higher solubility. At the same time, multi-stage regeneration units lead to a remarkable reduction of the thermal energy consumption, thus enhancing the process overall efficiency, though reducing the available driving force increasing the heat transfer area requirements.

The highest thermal efficiency around 13%, corresponding to an exergy conversion efficiency of about 50%, was observed for KAc and LiCl at molalities between 15 and 17 mol/kg_s, though the effect of molality becomes almost negligible above 10 mol/kg_s.

With this respect, operating at lower concentrations might lead to advantages in terms of better performance of the actual ion exchange membranes, which are known to lose significantly permselectivity when solute concentration increases above 5-10 M. This points to the fact that specific interactions between salt solutions-membranes can be the real controlling aspects in the performance enhancement of this technology, thus requiring a closer consideration of the most recent advances in IEMs technology and their future perspectives.

5.3 NOMENCLATURE

a	Activity (mol/kg$_s$)
AD	Adsorption Desalination
AEM	Anionic Exchange Membrane
A_ϕ	Debye-Huckel parameter for the osmotic coefficient
b	Constant parameter 1.2 kg$^{1/2}$·mol$^{-1/2}$
b_{01}, b_{02}	Fitting coefficients for the first parameter of second virial coefficient
b_{11}, b_{12}	Fitting coefficients for the second parameter of second virial coefficient
B_{MX}	Second viral coefficient
C_{MX}	Third virial coefficient
BPE	Boiling point elevation
c_1, c_2	Fitting coefficients for the third virial coefficient
$CAPMIX$	Capacitive mixing
CEM	Cation Exchange Membrane
CsAc	Caesium acetate
e	Electron charge (C),
$e.m.f.$	Electro-motive force (V)
f	Fugacity (bar)
G	Gibbs free energy (J)
HE	Heat Engine
I	Ionic strength (mol/kg$_s$)
k	Boltzmann's constant (J/K)
KAc	Potassium acetate
LiBr	Lithium bromide
LiCl	Lithium chloride
m	Molality (mol/kg$_s$)
m_0	Standard molality (mol/kg$_s$)
MD	Membrane Distillation
MED	Multi Effect Distillation
MW	Molecular weight (g/mol)
n	Moles (mol)
N_0	Avogadro's Number (kmol^{-1})
N_{stages}	Number of stages of the evaporative regeneration unit
NaAc	Sodium acetate
NaCl	Sodium chloride
OCV	Open circuit voltage (OCV)
p	Vapour pressure (bar)
PRO	Pressure Retarded Osmosis
	Thermal energy (J)

R	Universal gas constant (J/ (mol K))
RED	Reverse electrodialysis
SGP	Salinity Gradient Power
T	Temperature (°C or K)
T_c	Critical temperature (K)
TEC	Thermal energy consumption (J)
w	mass of solution (kg)
z	Ion charge (e)

Greek symbols

$\beta_{MX}^{(0)}$,	Parameter of second virial coefficient
$\beta_{MX}^{(1)}$	Parameter of second virial coefficient
ϵ_0	permittivity of free space ($F \cdot m^{-1}$)
λ_{ev}	Enthalpy of vaporization (kJ/kg)
μ	Chemical potential (J/mol)
ΔT	Temperature difference [°C or K]
α	Numerical constant
ΔG_{mix}	Gibbs free energy of mixing (J)
γ	Activity coefficient (dimensionless)
ϵ	Relative permittivity of water
η	Efficiency (dimensionless)
ν	Number of ions
ρ	Density (kg/m^3)
ϕ	Osmotic Coefficient (dimensionless)

Superscripts

0	Reference state
$+$	Related to positive ion
$-$	Related to negative ion
ϕ	Related to the osmotic coefficient
γ	Related to the activity coefficient
eb	Related to boiling conditions
$cond$	Related to the condensing vapour

Subscripts

$\pm$	Geometrical average between ions of an electrolyte solution
ex	Related to Exergy
$exch$	Related to the heat exchanger
$high$	High concentration stream
i	Generic species
in	Related to the inlet solution

k	Related to the generic evaporative stage
low	Low concentration stream
M	Related to the cation
mix	Related to the mixing solution
$multi$	Related to multi stage regeneration unit
MX	A generic 1-1 electrolyte
n	Related to normal conditions
out	Related to the outlet solution
$pure$	Related to pure solvent
s	Related to the solvent
$single$	Related to single stage regeneration unit
sol	Related to the solution
th	Thermal
w	Related to water
X	Related to the anion
γ	Related to the activity coefficient
ϕ	Related to the osmotic coefficient
vap	Related to the vapour

References

[1] S. Zhang, G. Han, X. Li, C. Wan, T.-S. Chung, 2 – Pressure retarded osmosis: Fundamentals, in: Sustain. Energy from Salin. Gradients, 2016: pp. 19–53. doi:10.1016/B978-0-08-100312-1.00002-X.

[2] F. Giacalone, A. Cipollina, F. Grisafi, A. Tamburini, G. Vella, G. Micale, Characterization of pressure retarded osmosis lab-scale systems, Desalin. Water Treat. 57 (2016) 22994–23006. doi:10.1080/19443994.2016.1173379.

[3] A. Cipollina, G. Micale, A. Tamburini, M. Tedesco, L. Gurreri, J. Veerman, S. Grasman, 5 – Reverse electrodialysis: Applications, in: Sustain. Energy from Salin. Gradients, 2016: pp. 135–180. doi:10.1016/B978-0-08-100312-1.00005-5.

[4] J. Veerman, D.A. Vermaas, 4 – Reverse electrodialysis: Fundamentals, in: Sustain. Energy from Salin. Gradients, 2016: pp. 77–133. doi:10.1016/B978-0-08-100312-1.00004-3.

[5] R. Rica, R. Ziano, D. Salerno, F. Mantegazza, R. van Roij, D. Brogioli, Capacitive Mixing for Harvesting the Free Energy of Solutions at Different Concentrations, Entropy. 15 (2013) 1388–1407. doi:10.3390/e15041388.

[6] A. Tamburini, M. Tedesco, A. Cipollina, G. Micale, M. Ciofalo, M. Papapetrou, W. Van Baak, A. Piacentino, Reverse electrodialysis heat engine for sustainable power production, Appl. Energy. 206 (2017) 1334–1353. doi:10.1016/j.apenergy.2017.10.008.

[7] M. Papapetrou, G. Kosmadakis, A. Cipollina, U. LaCommare, G. Micalea, Industrial waste heat: Estimation of the technically available resource in the EU per industrial sector, temperature level and country, Appl. Therm. Eng. Under Revi (2017). doi:10.1016/j.applthermaleng.2018.04.043.

[8] H.T. El-Dessouky, H.M. Ettouney, Fundamentals of Salt Water Desalination, 2002. doi:10.1016/B978-044450810-2/50008-7.

[9] A. Alkhudhiri, N. Darwish, N. Hilal, Membrane distillation: A comprehensive review, Desalination. 287 (2012) 2–18. doi:10.1016/j.desal.2011.08.027.

[10] C. Olkis, G. Santori, S. Brandani, An Adsorption Reverse Electrodialysis system for the generation of electricity from low-grade heat, Appl. Energy. (2018).

[11] M. Bevacqua, A. Tamburini, M. Papapetrou, A. Cipollina, G. Micale, A. Piacentino, Reverse electrodialysis with NH4HCO3-water systems for heat-to-power conversion, Energy. (2017). doi:10.1016/j.energy.2017.07.012.

[12] D. Lide, Aqueous Solubility of Inorganic Compounds at Various Temperatures, CRC Handb. Chem. Phys. (2005) 1–6. papers2://publication/uuid/55E853FE-9E62-4EEC-97D7-AFAB12AA3361.

[13] A. Tamburini, M. Tedesco, A. Cipollina, G. Micale, M. Ciofalo, M. Papapetrou, W. Van Baak, A. Piacentino, Reverse electrodialysis heat engine for sustainable power production, Appl. Energy. 206 (2017) 1334–1353. doi:10.1016/j.apenergy.2017.10.008.

[14] N.V. Sidgwick, J.A.H.R. Gentle, CCXXI.—The solubilities of the alkali formates and acetates in water, J. Chem. Soc., Trans. 121 (1922) 1837–1843. doi:10.1039/CT9222101837.

[15] D. Lide, Aqueous Solubility of Inorganic Compounds at Various Temperatures, CRC Handb. Chem. Phys. (2005) 1–6.

[16] J. Veerman, M. Saakes, S.J. Metz, G.J. Harmsen, Reverse electrodialysis: Performance of a stack with 50 cells on the mixing of sea and river water, J. Memb. Sci. 327 (2009) 136–144. doi:10.1016/j.memsci.2008.11.015.

[17] R. Long, B. Li, Z. Liu, W. Liu, Hybrid membrane distillation-reverse electrodialysis electricity generation system to harvest low-grade thermal energy, J. Memb. Sci. (2016). doi:10.1016/j.memsci.2016.10.035.

[18] J. Hu, S. Xu, X. Wu, D. Wu, D. Jin, P. Wang, Q. Leng, Theoretical simulation and evaluation for the performance of the hybrid multi-e ff ect distillation — reverse electrodialysis power generation system, 443 (2018) 172–183. doi:10.1016/j.desal.2018.06.001.

[19] K.S. (Kenneth S. Pitzer, Activity coefficients in electrolyte solutions, CRC Press, 1991.

[20] K.S. Pitzer, J.C. Peiper, R.H. Busey, Thermodynamic Properties of Aqueous Sodium Chloride Solutions, J. Phys. Chem. Ref. Data. 13 (1984) 1–102. doi:10.1063/1.555709.

[21] H.F. Gibbard Jr, G. Scatchard, Liquid-vapor equilibrium of aqueous lithium chloride, from 25 to 100. deg. and from 1.0 to 18.5 molal, and related properties, J. Chem. Eng. Data. 18 (1973) 293–298. doi:10.1021/je60058a011.

[22] K.R. Patil, A.D. Tripathi, G. Pathak, S.S. Katti, Thermodynamic Properties of Aqueous Electrolyte Solutions. Vapor Pressure of Aqueous Solutions of LiCI, LiBr, and LiI 1, J. Chem. Eng. Data. 35 (1990) 166–168. doi:10.1021/je00060a020.

[23] D.G. Archer, Thermodynamic propertis of the KCl + H2O system, J. Phys. Chem. Ref. Data. 28 (1999) 1–16. doi:10.1063/1.556034.

[24] R. Beyer, M. Steiger, Vapour pressure measurements and thermodynamic properties of aqueous solutions of sodium acetate, J. Chem. Thermodyn. 34 (2002) 1057–1071. doi:10.1006/jcht.2002.0974.

[25] R.A. Robinson, The Osmotic and Activity Coefficient Data of Some Aqueous Salt Solutions from Vapor Pressure Measurements, J. Am. Chem. Soc. 59 (1937) 84–90. doi:10.1021/ja01280a019.

[26] R. Robinson, The Activity Coefficients of Alkali Nitrates, Acetates and p-Toluenesulfonates in Aqueous Solution from Vapor Pressure Measurements, J. Am. Chem. Soc. 57 (1935) 1165–1168. doi:10.1021/ja01310a005.

[27] W.J. Hamer, Y. Yung chi, Osmotic Coefficients and Mean Activity Coefficients of Uni univalent Electrolytes in Water at 25??C, J. Phys. Chem. Ref. Data. 1 (1972) 1047–1100. doi:10.1063/1.3253108.

[28] D.J. Bradley, Thermodynamics of Electrolytes. 12. Dielectric Properties of Water and Debye-Huckel Parameters to 350, 83 (1979).

[29] F. Giacalone, P. Catrini, A. Tamburini, A. Cipollina, A. Piacentino, G. Micale, Exergy analysis of reverse electrodialysis, Energy Convers. Manag. 164 (2018) 588–602. doi:10.1016/j.enconman.2018.03.014.

[30] N.Y. Yip, M. Elimelech, Thermodynamic and energy efficiency analysis of power generation from natural salinity gradients by pressure retarded osmosis, Environ. Sci. Technol. 46 (2012) 5230–5239. doi:10.1021/es300060m.

[31] A. Saul, W. W., International Equations for Saturation Properties of Ordinary Water Substance, J. Phys.Chem. Ref. Data. 16 (1987). doi:10.1063/1.555926.

[32] R.M. S., Coulson and Richardson's Chemical Engineering Volume 6 (Design), 2nd Edition, by R.K. Sinnott, Pergamon Press, Oxford, UK (1993). 954 pages. ISBN 0-08-041865-1., Dev. Chem. Eng. Miner. Process. 2 (2008) 254–255. doi:doi:10.1002/apj.5500020410.

[33] A. Carati, M. Marino, D. Brogioli, Thermodynamic study of a distiller-electrochemical cell system for energy production from low temperature heat sources, Energy. 93 (2015) 984–993. doi:10.1016/j.energy.2015.09.108.

[34] N. Hubert, Y. Gabes, J. Bourdet, L. Schuffenecker, Vapor Pressure Measurements with a Nonisothermal Static Method between 293.15 and 363.15 K for Electrolyte Solutions. Application to the H2O + NaCl System, J. Chem. Eng. Data. 40 (1995) 891–894. doi:10.1021/je00020a034.

[35] Mokbel, I, Ye, S, Jose, J, Xans, P, Study of non ideality of various aqueous sodium chloride solutions by vapor pressures measurements and correlation of experimental results by Pitzer's method, J. Chim. Phys. 94 (1997) 122–136. doi:10.1051/jcp/1997940122.

APPENDIX

A.1. Validation of the experimental methodology

The thermocouple used to evaluate the solution temperature is in a glass branch not directly in contact with the liquid. Therefore, in order to overcome the uncertainty of the sensor, the cell was first calibrated against water vapour pressures [31]. Figure A.1 shows the comparison of the temperature measured using the thermocouple and the actual boiling temperature of the solution. The equation used to correct the measured values is also reported in the same figure.

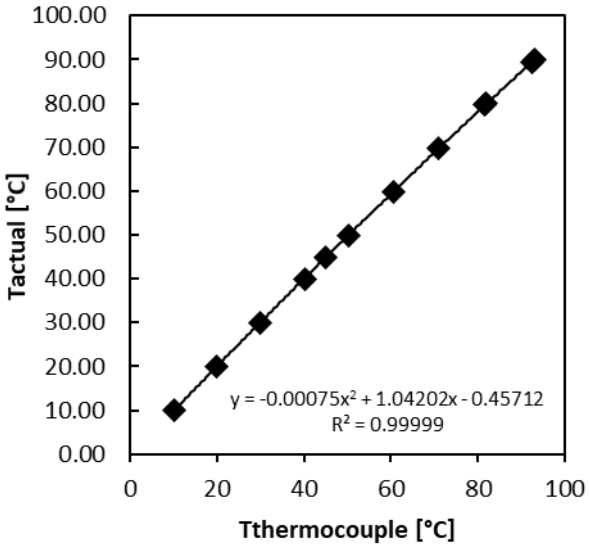

Fig. A. 1 *Temperature calibration curve of the thermocouple*

In order to validate the overall methodology of extracting the model parameters from the vapour pressure data, partial pressure measurements for NaCl- and LiCl- water solutions were compared with literature data at different temperature and pressure, as reported in Table A1.

Table A. 1 *Comparison of experimental partial pressure of NaCl solutions measured in this work and literature data* [34,35] *at different temperature and molality.*

This work			**Literature** [34]		
m [mol/kg$_s$]	**T [°C]**	**p [kPa]**	**m [mol/kg$_s$]**	**T [°C]**	**p[kPa]**
1.032	10.0	1.19	1.029	10.4	1.22
1.032	20.0	2.27	1.029	20.4	2.32
1.032	30.0	4.11	1.029	30.8	4.18
1.032	39.9	7.09	1.029	40.1	7.17
1.032	49.9	11.85	1.029	50.1	11.99
1.032	59.9	19.18	1.029	60.1	19.38
1.032	69.8	29.72	1.029	70.2	30.34
1.032	79.7	45.09	1.029	80.1	45.76
2.040	10.3	1.16	2.034	10.4	1.17
2.040	20.1	2.19	2.034	20.4	2.20
2.040	30.1	3.97	2.034	30.2	3.98
2.040	39.9	6.85	2.034	40.2	6.92
2.040	49.9	11.41	2.034	50.1	11.49
2.040	59.9	18.43	2.034	60.1	18.59
2.040	69.8	28.78	2.034	70.0	28.98
2.040	79.7	43.38	2.034	80.0	43.87
2.040	89.6	63.94	2.034	90.0	64.85
3.131	10.1	1.10	3.141	10.4	1.12
3.131	20.0	2.09	3.141	20.4	2.12
3.131	30.0	3.79	3.141	30.2	3.80
3.131	39.9	6.54	3.141	40.2	6.58
3.131	50.0	10.96	3.141	50.2	10.95
3.131	59.9	17.52	3.141	60.1	17.73
3.131	69.8	27.37	3.141	70.1	27.67
3.131	79.7	41.35	3.141	80.1	41.93
3.131	89.4	61.00	3.141	90.0	62.01
5.424	20.0	1.84	5.423	21.3	1.99
5.424	30.1	3.34	5.423	30.9	3.50
5.424	40.0	5.80	5.423	40.5	5.94
5.424	50.0	9.69	5.423	50.3	9.79
5.424	59.9	15.49	5.423	60.1	15.73

Table A. 2 *Comparison of experimental partial pressure of LiCl solutions measured in this work and literature data* [22] *at different temperature and molality.*

This work			**Literature** [22]		
m [mol/kg$_s$]	**T [°C]**	**p [kPa]**	**m [mol/kg$_s$]**	**T [°C]**	**p[kPa]**
3.001	30.1	0.037	3.01	30	0.0368
3.001	40.0	0.0645	3.01	40	0.0642
3.001	50.0	0.1081	3.01	50	0.1078
3.001	59.9	0.1743	3.01	60	0.1747
3.001	69.9	0.2725	3.01	70	0.2741
6.0018	30.2	0.0293	5.998	30	0.0289
6.0018	40.1	0.051	5.998	40	0.0506
6.0018	50.0	0.085	5.998	50	0.0851
6.0018	60.0	0.1384	5.998	60	0.1382
6.0018	69.8	0.2157	5.998	70	0.2175
10.1829	30.0	0.0169	10.168	30	0.0172
10.1829	40.0	0.0302	10.168	40	0.0307
10.1829	50.0	0.0519	10.168	50	0.0527
10.1829	60.0	0.0861	10.168	60	0.087
10.1829	69.8	0.1368	10.168	70	0.1393

A comparison of osmotic coefficients obtained from experimental measurements of solution vapour pressure for Sodium Chloride, (ii) Lithium Chloride and (iii) Sodium Acetate water solutions and the ones obtained using literature models is reported in figure A.1. The modelling osmotic coefficients refer to calculated values obtained using literature virial coefficients (Pitzer's model), as in the case of NaCl [20] and $NaC_2H_3O_2$ [24], or fitting available literature model for osmotic coefficients, as in the case of LiCl [21]. For each salt, several molalities and solution temperatures were analysed.

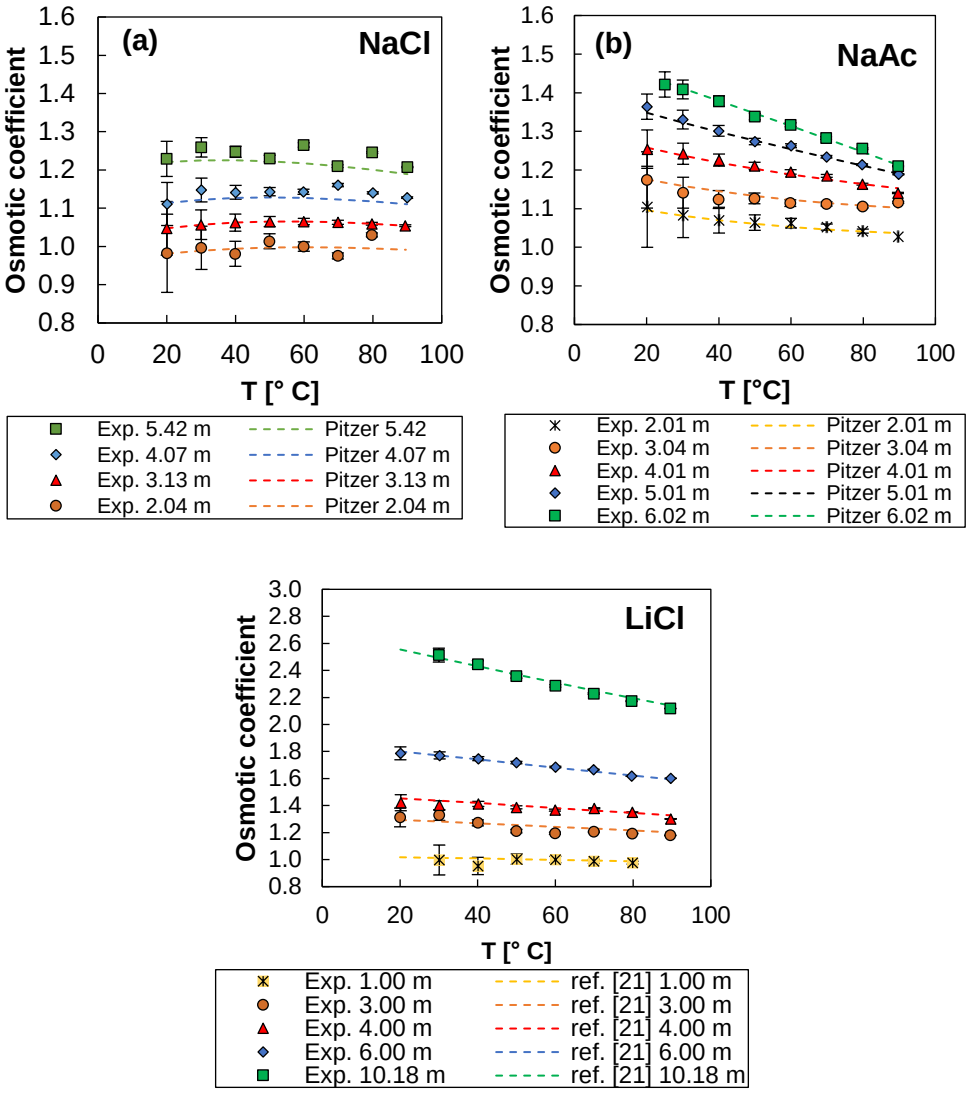

Fig. A. 2.*Comparison between experimental and model osmotic coefficient for NaCl (a), NaAc (b) and LiCl (c) as a function of molality and solution temperature. Pitzer's coefficients from literature date* [20–22,24].

At low concentration and temperature (or vapour pressure) the relative experimental error increases. The error

633 bars in the figures are evaluated according to the expression:

634 $$\Delta\phi = \frac{-1000}{2MWm}\frac{\Delta p}{p} \quad (18)$$

635 a very small deviation in vapour pressure can lead to an important deviation in ϕ, when the molality m tends
636 to zero [34].This means that the evaluation of experimental virial coefficients through experimental osmotic
637 coefficients with the proposed test rig can be done with a low error at concentrations above 2 molal and
638 temperatures higher than 20°C, which are the conditions of interest in this study.

639 ## A.2. Boiling point elevation

640 Figure A.2 reports the comparison of calculated and experimental BPE for NaCl, NaAc and LiCl water
641 solutions, confirming that the values obtained from the experimental apparatus are sufficiently accurate to
642 determine the theoretical efficiency of the regeneration process.

643

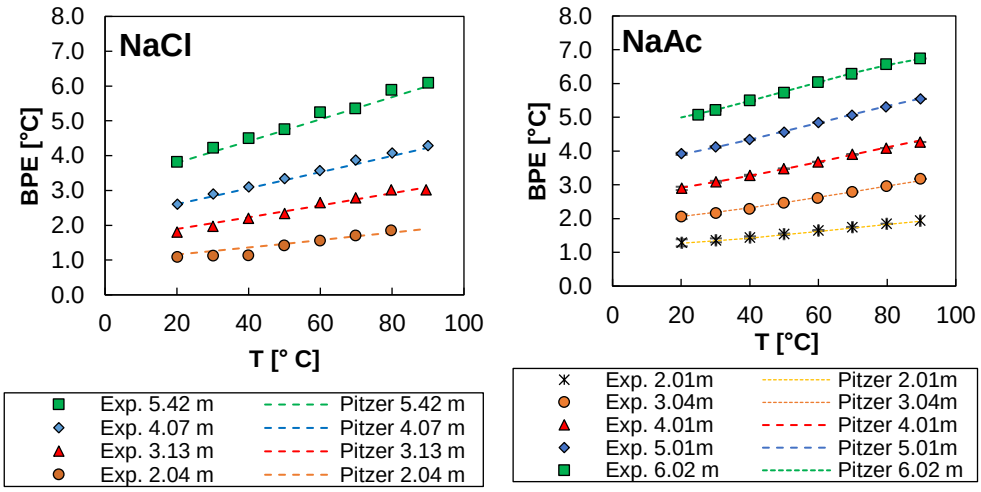

644

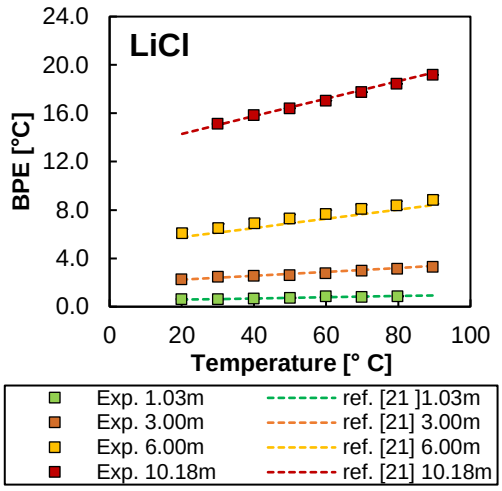

645

646 ***Fig. A.* 3.** *Calculated and experimental BPEs as function of molality and temperature for NaCl, NaAc and LiCl.*

647

648